INTL JOURNAL OF ELECTRONICS AND TELECOMMUNICATIONS, 2020, VOL. 68, NO. 3, PP. 641–646
Manuscript received November 20, 2021; revised August, 2022. DOI: 10.24425/ijet.2022.141284

Palmprint Recognition Using Gabor-Based Scale Orientation

Muhammad Kusban

***Abstract*—Various methods are used to obtain a superior palmprint recognition system. After selecting a palmprint image filter, using Gabor orientation scale pairs is an option to support the refinement of the verification process. Many researchers use the $[8 \times 5]$ pair for the value of the Gabor orientation scale in the field of palmprint recognition. However, from the experiments conducted, other Gabor pairs have more impact on system improvement. The problem is to get the most suitable value pairs for palmprint applications, so in this study, a comparison of seven kinds of Gabor pairs is carried out. This Gabor pair being compared applies using original images, PCA dimension reduction, and the Euclidean method. From the research that has been done, the pair of Gabor orientation scale $[8 \times 7]$ or image expansion of 56 will have the most significant impact compared to other pairs. Suppose the result of this Gabor pair is $[8 \times 7]$ by using other improvement systems, namely the 3W filter instead of the original image, KPCA to replace the PCA, and the cosine method in the matching method. In that case, it will increase the verification value by 99.611%. The trial value obtained can be an alternative method of choice for improving palmprint recognition.**

***Keywords*—Scale orientation Gabor, Palmprint recognition, verification and equal error rate, four biometric curves, KPCA**

I. Introduction

THE use of biometric systems as an identification system has increased, one of which is the palm. The palm print is a relatively new biometric with the unique characteristic of stable palm lines. The uniqueness and stability of these hand lines are reliable features of each palm. Palm biometrics has the advantage of relatively larger dimensions than fingerprint biometrics, and the detection process can be done without attaching it to a scanner. Thus, detecting people can be carried out quickly and bulk by simply waving their hands. So this system is suitable when applied at the airport. Outline researchers in the field of palmprint recognition have divided the research subsection into four parts, namely preprocessing, homogeneity of image position, dimension reduction, and matching techniques [1]–[3]. If the research emphasizes the search for characteristics in the form of the main line of the palm, then the acquisition tool to get a digital image is enough to use a camera or web camera. The results of the image acquisition then produce an ROI image. The research series can start and end with this form when the EER value, verification, and curve display are obtained. From each method used, the research aims to get the lowest possible EER value. The low value of EER will be closely related to the superiority of system performance, namely a high verification value.

After normalizing the image, it is necessary to homogenize the reference points and reduce the amount of data that is not important. Both processes are in one group, namely in the data extraction section. As an alternative to data extraction applications, the use of the Legendre moment method cannot be applied in the normalization process if all images are not oriented in the same direction [4]. However, if using another method, namely Gabor, it can be used to normalize the position of various [5] images. Along with the opinion of this researcher, other researchers stated that the use of Gabor also strengthens the information feature of [6]. The opinion of the two researchers was strengthened by the third researcher, who stated that the PCA and Gabor $[6 \times 3]$ methods were able to improve the system performance of [7]. Thus, combining Gabor $[8 \times 5]$ and PCA dimension reduction can yield a verification value above 95% [8]. In addition to using PCA, other methods, namely KPCA and the Gabor $[8 \times 5]$ scale orientation, can produce a good performance [9]. Researchers have widely used use pairs of Gabor orientation scales. However, until now, there is still no definite choice that everyone can accept. Using the PolyU database for ROI *original* and combining the Gabor method worth $[8 \times 5]$ a verification value of 97.12% will be generated using PCA dimension reduction and Euclidean is matching [9]. Using the *morphology* filter for image improvement and the Gabor technique of $[8 \times 5]$, then using the PCA method and the Hamming technique for matching will be able to produce $95,409\%$ of a verification value [8]. Furthermore, improvements to the palmprint recognition system with a binary filter and the Gabor method for $[6 \times 3]$ will produce a system with an error rate of 3%. The achievement of this value when cooperating with PCA technique as a means of dimension reduction and matching technique *weight sum* [7]. Finally, other researchers used the *skeleton* method for the image enhancement process, continued to use Gabor $[6 \times 6]$, and the multiple-machers matching method managed to get a value of 0.18% for the error-rate [10]. Regarding the use of the Gabor procedure, one researcher stated that to improve system performance is not only based on the selection of scale orientation pairs but can be achieved by using the initial value of the Gabor scale parameter or orientation [11]. Other researchers strengthened this opinion by suggesting that four constant values in the Gabor core should be selected for the

Muhammad Kusban is with Faculty of Electrical Engineering, Universitas Muhammadiyah Surakarta, Pabelan, Indonesia (e-mail: Muhammad.Kusban@ums.ac.id).

success of the palmprint system [6]. After the data was swelled by applying the Gabor technique, the process was continued with a dimension reduction system. Many researchers suggest the use of PCA. However, this principle can be refuted because PCA is not suitable for the biometric fusion process because it is not efficient in computing [12]. This fact is supported by other researchers who assert that the use of PCA is only able to retrieve information patterns of low-dimensional data [13].

The output data that has been obtained is then processed in the matching segment, namely the calculation of the distance value between *training* and *testing*. The matching method that researchers in the field of biometrics widely use is the Euclidean [14] method. The advantages of using the Euclidean technique are: the simplicity of function, ability to find a unique scope of solutions, and excels in solving far different models [15]. In addition, there is evidence that by using Euclidean in one of its biometric methods, obtain above 97% for verification performance [9]. Of all the advantages that have been mentioned, it turns out that the Euclidean method has a weakness, namely the lack of anticipation of input data that has unequal attributes [16]. From the conclusion of all the research results that have been tabulated, it can be concluded that obtaining a superior information style can be achieved by combining three methods. The first is the information pattern of the Gabor method, the design generated from the PCA method (*principal component analysis*). The last is the combination of the three ways of information originating appearance, outline, and texture. The three types of information patterns are then combined using a fusion mechanism. The final output of the fusion is a genuine and imposter [17] image. Differences of opinion between researchers continue to this day so that the use of the palmprint recognition method continues to develop with guidelines for four topics, namely the use of image filters, the use of the Gabor orientation scale, the choice of dimension reduction techniques, and finally the selection of matching methods. Primarily based on the Gabor scale and orientation passage, researchers have not widely studied and still have opportunities to be developed.

II. Theory

The ability of the human visual system to distinguish various textures is based on the ability to identify multiple frequencies and spatial orientations of the observed texture. Gabor Filter is a filter that can simulate the characteristics of the human visual system by isolating specific frequencies and directions from the image. These characteristics make the Gabor filter suitable for texture recognition applications in computer vision. The Gabor filter is a linear filter used in biometric feature extraction as a feature detector. Gabor filter is a successful feature detector because it can eliminate variability caused by contrast illumination and slight shift and deformation of the image. Gabor filter output has been used successfully for face detection [18]–[20] dan palmprint recognition [21], [22]. The weakness of the Gabor method is the increased amount of data, so the computational process rises. The Gabor procedure is a linear filter for edge-detection, resulting from the convolution between a sine wave and a Gaussian function. Since it is obtained from the convolution product, then The resulting output is a Fourier function of complex form. The property of the Fourier function is non-stationary. To obtain the pattern of information for the desired time cannot use because there is no localization in time. On the other hand, although the short-time *windowed Fourier transform* method can obtain information in the desired time, the value obtained remains the same because there is no difference between the time and frequency phases. To overcome this problem, the Gabor technique is applied with the aim of obtaining information in the *windowed Fourier Transform* of the phase differences that occur. The value obtained from the Gabor process is also known as local value. Said by Štruc that local value has a value range of $[t_0 \pm \sigma_c \times \omega_0 \pm \sigma_c]$ with t_0 the time when $t = 0$, $\omega_0 = 2\pi f$, and σ_c the midpoint of *square window* between time and frequency [23]. In applications, the Gabor filter is a Morlet shape wavelet to reduce the standard deviation in the time and frequency domains. This subtraction is identical to trying to reduce the unimportant information of the variance and arithmetic-mean values. To get an illustration of the use of the two Gabor variables and the resulting display impact, the figure 1 shows the results obtained from the orientation process and the Gabor technique scale of 40 variation. Many researchers use the Gabor orientation scale to reference image position [4], [5], [24]. Besides being used for reference values, another added advantage is the ability to get important information at different times due to differences in orientation direction and the size of the scale used. This principle is an extension of what cannot be obtained in the *the windowed short-time Fourier transform* method.

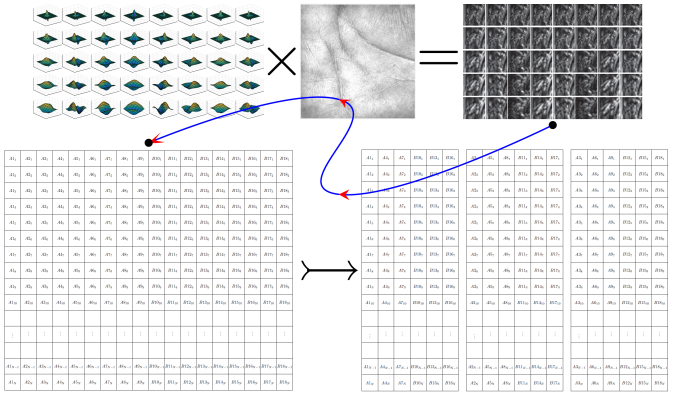

Fig. 1. Illustration of Gabor scale orientation for 40 changes

The Gabor method is generally used to obtain the normalization of the angle and the scale difference of the image data. Output from the Gabor method has value as much as the multiplication of the orientation parameter with the scale. The thousands of image data used for the input process require normalization in terms of scale and image orientation. The use of the *Legendre Moment* method from previous researchers has a weakness. Namely, it fails to process images that are not oriented in the same direction. These weaknesses can be overcome by using the Gabor method. The Gabor method improves performance when it has the correct multiplication pair between orientation and scale. The Gabor equation contains

various parameters. If a particular constant value can reduce these parameters, it is sure to speed up the process. A system sometimes gets optimal performance through an unordered selection of parameters. The effectiveness of the gray level information from the co-occurrence matrix can be increased by selecting *entropy based jets* which are not sequential [25]. From the results of this study, it can be Based on the idea of [25], Other researchers concluded that a particular value jump method is needed for the order of the Gabor value of scale and orientation. Another researcher states that system performance through the Gabor filter can be improved if the initial use of the scale value (ς) or orientation (ϑ) does not start at 0 but starts at 2 and sort in increments of $\sqrt{2}$ [11]. So for example $\varsigma = 8, \vartheta = 7$ then the increase in the value of the loop is $\varsigma = [0, 1, 2, 3, 4, 5, 6, 7]$ and $\vartheta = [2, 2\sqrt{2}, 4, 4\sqrt{2}, 8]$. Furthermore, in specific applications involving the Gabor technique, four components can be adjusted to get optimal results [6]. The four variables are sequentially notated: *entropy* ($\mathcal{E}$), *variance* ($\mathcal{V}$), *energy* ($\mathcal{F}$), and *dissimilarity* (Δ). The general equation for the complex Gabor function G is the product of the sinusoidal carrier ($\mathcal{S}$) by the Gaussian envelope ($\mathcal{G}$), which can be expressed in the following form.

$$G(x, y) = \mathcal{S}(x, y)\mathcal{G}(x, y). \tag{1}$$

With a different form of notation, other researchers state that the basis of the Gabor equation ($G_{\varsigma,\vartheta}$) is the product of a sine wave (S) with a Gaussian exponential function (Γ). The equation by Štruc can be expressed as follows [23].

$$G(\varsigma, \vartheta) = S \times \Gamma = \frac{f_u^2}{\pi\vartheta\eta} e^{-\left[\left(\frac{f_u^2}{\vartheta^2}\right)\hat{x}^2 + \left(\frac{f_u^2}{\eta^2}\right)\hat{y}^2\right]} e^{j2\pi f_u \hat{x}}, \tag{2}$$

with $\hat{x} = x\cos\varsigma_v + y\sin\varsigma_v$, $\hat{y} = -x\sin\varsigma_v + y\cos\varsigma_v$, $f_u = f_{\max}/2^{u/2}$, and $\varsigma_v = v\pi/8$. The notation f_u for the center frequency and ς_v for the orientation direction, ϑ for the center frequency ratio, and η for the Gaussian envelope size.

The equation (2) is in complex form. The separation in real ($\Re_G$) and imaginary ($\Im_G$) forms with a fixed orientation direction is as follows.

$$\begin{aligned} \Re_G(\varsigma, \vartheta) &= \exp\left[-\frac{\hat{x}^2 + \gamma^2\hat{y}^2}{2\sigma^2}\right]\cos\left(2\pi\frac{\hat{x}}{\lambda} + \gamma\right) \\ \Im_G(\varsigma, \vartheta) &= \exp\left[-\frac{\hat{x}^2 + \gamma^2\hat{y}^2}{2\sigma^2}\right]\sin\left(2\pi\frac{\hat{x}}{\lambda} + \gamma\right), \end{aligned} \tag{3}$$

where $\hat{x} = x\cos\varsigma + y\sin\varsigma$ and $\hat{y} = -x\sin\varsigma + y\cos\varsigma$. Real values are more often chosen to get important information than imaginary values. However, the absolute value is more widely used by researchers. The absolute value of $\hat{G}(\varsigma, \vartheta)$ and the phase $\varphi(\varsigma, \vartheta)$ can be obtained from Equation (3) in the following form.

$$\begin{aligned} \hat{G}(\varsigma, \vartheta) &= \sqrt{[\Re_G(\varsigma, \vartheta)]^2 + [\Im_G(\varsigma, \vartheta)]^2} \\ \varphi(\varsigma, \vartheta) &= \arctan\frac{\Im_G(\varsigma, \vartheta)}{\Re_G(\varsigma, \vartheta)} \end{aligned} \tag{4}$$

The Gabor method is used to normalize various images that have non-uniform orientation angles and scales. The test image has various sizes, so it is necessary to have the same size. If the image size is $[ab]$, then for computational convenience and uniformity between different data, then choose the same size $[nn]$. This study chooses the image size $[128128]$ to represent its information. Because the Gabor method has sin and cos values with a range of positive and negative values for one cycle, the image size is multiplied twice, stretching from $-n$ to $(n-1)$, becoming $[256256]$. Then together with the four parameters whose values are set, namely $f_{\max}, \mathcal{F}, \mathcal{E}, \Delta$ will get the Gabor value. The selection of these values is based on several tests shown in table III. The output from Gabor is what then separates the data between the three classifications of test data: *training*, *testing*, and *evaluating*. When using the Gabor matrix $[16, 16]$, the length of the classification of the test data is $[16 \times 16 \times 8 \times 5]$ with a scale value of $\varsigma = 8$ and an orientation of $\vartheta = 5$. The value used in the separation of the resulting matrix classification for *training, testing* and *evaluating* is $[3 \times i]$ with a value of three as the image variation and i is the number of research samples.

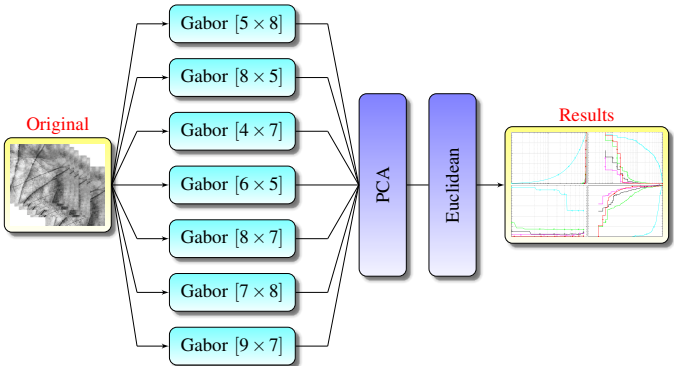

Fig. 2. Gabor scale and orientation selection flowchart

III. Experiment

The study used data from the PolyU database of as many as 600 items. Each item has a variation of 10 images. The source of the database is open-access, which can compare the research results with other researchers' output. The study used a value of three for *training* and *testing*, while *evaluating* used the remaining value of 4. The Gabor parameter experiment is used to get the best value for image stability when there is a change in scale and orientation. In this study using seven kinds of Gabor parameter choices. The sequence of work steps is displayed in flowchart Image 2. The research results are written in the I and II Tables. The curve display is in Image 3 - 4. The research process uses the original image, Gabor $[8 \times 5]$, PCA dimension reduction, and finally, the matching method with the Euclidean technique. The I table shows the research output, while the 3 shows the biometric ROC curve as an explanation of the resulting research output. From Table I shows that the highest verification value of $98,944\%$ and an EER error rate of $1,057\%$ occurred in the orientation scale pair of $\varsigma = 8, \vartheta = 7$. The red line represents the value of $\varsigma = 8, \vartheta = 7$ in the image 3, highlighting the advantages of this Gabor value pair over other value pairs. From the seven curve lines, it can be seen that the red line has the smallest *false accept rate* value of 0 and the highest *false rejection rate* value is 1.

TABLE I
THE RESULTS OF THE STUDY USING THE ORIGINAL IMAGE, THE GABOR VALUE $[8 \times 5]$, PCA DIMENSION REDUCTION, AND THE EUCLIDEAN MATCHING METHOD

Gabor	$\mathcal{RD}$	EER	Time	FRR	Ver.	FAR
5×8	PCA	2.051	5.17281	0.02056	97.944	0.02045
8×5	PCA	1.164	5.09877	0.01167	98.833	0.01161
4×7	PCA	1.834	4.32634	0.01833	98.167	0.01836
6×5	PCA	1.556	4.45434	0.01556	98.444	0.01555
8×7	PCA	1.057	6.18340	0.01056	98.944	0.01059
7×8	PCA	1.268	6.24552	0.01278	98.722	0.01259
9×7	PCA	1.093	6.81513	0.01111	98.889	0.01074

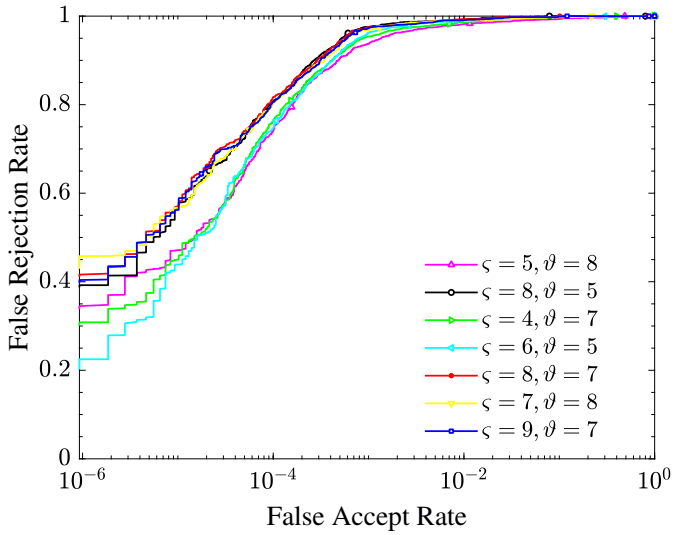

Fig. 3. ROC curve that shows the comparison of research outcomes with 500 items of data and the use of PCA and Euclidean

In follow-up research, activities are centered on changing Gabor parameters and matching methods. The II table shows the results of further research while maintaining the seven variables of the Gabor orientation scale. The variables used are the ThreeW filter to replace the original image and the cosine method for matching techniques. The Gabor orientation scale and reduction methods remain the same from previous studies. The LDA dimension reduction method dominates the acquisition of research values with the EER and verification error values of 0.278% and 99.722%. But looking at the largest processing time or computation time, the LDA method can be ignored. Furthermore, from the KPCA method, the orientation scale value pair of 8×7 outperformed the pair ς and ϑ. Likewise for PCA, the choices $\varsigma = 8, \vartheta = 7$ outperformed the other pairs of Gabor orientation scales.

It can be seen from the image 4 that the pair $\varsigma = 8, \vartheta = 7$ with a red line presentation, excels for the CMC, EPC, and ROC curves. It is clear that the CMC 4 curve (a) the red line has a *recognition rate* nearly 1 all in all. Then the pair $[\varsigma = 8 \times \vartheta = 7]$ in the image EPC curve 4 (c) shows that it has the lowest *error rate* value. Meanwhile, in the ROC curve of the image 4 (d) the red line dominates the advantage with other colors with the *false accept rate* approaching 1 and the *false rejection rate* approaching 0. For KPCA, the highest

TABLE II
RESULTS OF RESEARCH USING THREEW FILTERED DATA AND COSINE MATCHING TECHNIQUES IN FOUR-DIMENSIONAL REDUCTION BASES AND SEVEN GABOR PAIRS

Gabor	$\mathcal{DR}$	Time	FAR	FRR	EER	Ver.
5×8	KFA	3.46918	0.04952	4.944	0.04948	95.056
8×5	KFA	3.51801	0.34207	34.167	0.34187	65.833
4×7	KFA	3.43802	0.11101	11.056	0.11078	88.944
6×5	KFA	3.06052	0.05345	5.333	0.05339	94.667
8×7	KFA	3.27774	0.08935	8.944	0.08940	91.056
7×8	KFA	3.76340	0.11807	11.833	0.11820	88.167
9×7	KFA	3.68267	0.19621	19.667	0.19644	80.333
5×8	KPCA	2.88893	0.00831	0.833	0.00832	99.167
8×5	KPCA	2.71903	0.00565	0.556	0.00560	99.444
4×7	KPCA	2.45626	0.01022	1.000	0.01011	99.000
6×5	KPCA	2.54562	0.00907	0.889	0.00898	99.111
8×7	KPCA	2.64090	0.00388	0.389	0.00388	99.611
7×8	KPCA	2.77566	0.00499	0.500	0.00499	99.500
9×7	KPCA	2.68759	0.00499	0.500	0.00499	99.500
5×8	LDA	7.87819	0.00554	0.556	0.00555	99.444
8×5	LDA	7.59638	0.00388	0.389	0.00388	99.611
4×7	LDA	5.50663	0.00884	0.889	0.00886	99.111
6×5	LDA	5.80031	0.00886	0.889	0.00888	99.111
8×7	LDA	8.53836	0.00333	0.333	0.00333	99.667
7×8	LDA	9.09606	0.00278	0.278	0.00278	99.722
9×7	LDA	9.35421	0.00334	0.333	0.00334	99.667
5×8	PCA	5.70652	0.00972	1.000	0.00986	99.000
8×5	PCA	5.85832	0.00721	0.722	0.00722	99.278
4×7	PCA	4.40819	0.01032	1.000	0.01016	99.000
6×5	PCA	4.54485	0.00889	0.889	0.00889	99.111
8×7	PCA	5.92817	0.00556	0.556	0.00556	99.444
7×8	PCA	6.31833	0.00598	0.611	0.00605	99.389
9×7	PCA	6.18710	0.00575	0.556	0.00565	99.444

verification value is 99.611% and the EER error rate is 0.388% with a processing time of 2.64090 seconds.

TABLE III
TRIAL OF VARIOUS PARAMETERS IN THE GABOR METHOD FOR SCALE ORIENTATION $[8 \times 5]$

Parameter	EER	Ver.
$0 \rightarrow [\{x, y\} - 1]$	4.043	95.944
$-\{x, y\} \rightarrow [\{x, y\} - 1]$	1.168	98.833
$f_{\max}, \mathcal{E}, \mathcal{V},$ and $\Delta \rightarrow \sqrt{2}$	2.054	97.944
$f_{\max}, \mathcal{E}, \mathcal{V},$ and $\Delta \rightarrow 2$	1.122	98.889
$\mathcal{E}, \mathcal{V},$ and $\Delta \rightarrow \sqrt{2}, f_{\max}, \rightarrow 0,5$	2.054	97.944
$\mathcal{E}, \mathcal{V},$ and $\Delta \rightarrow \sqrt{2}, f_{\max}, \rightarrow 0.25$	2.054	97.944
$f_{\max}, \mathcal{E}, \mathcal{V},$ and $\Delta \rightarrow 5$	3.946	96.056
$f_{\max}, \mathcal{E}, \mathcal{V},$ and $\Delta \rightarrow 2,5$	1.208	98.778
$f_{\max}, \mathcal{E}, \mathcal{V},$ and $\Delta \rightarrow 1,5$	1.724	98.278

Furthermore, to make more use of the Gabor technique, can do alternate variable value settings. The value changes that have a significant impact on value changes are when setting the distribution of $f_{\max}, \epsilon, \mathcal{V}$ and Δ values. For the Gabor $[8 \times 5]$, original, PCA, and Euclidean pairs of 500 data objects, assigning these four variables with a value of 2 will produce the best outcome.

IV. CONCLUSION

By adjusting the choice of image filters, selecting Gabor orientation scale pairs, dimensional reduction methods, and appropriate matching techniques, it will get reliable palmprint

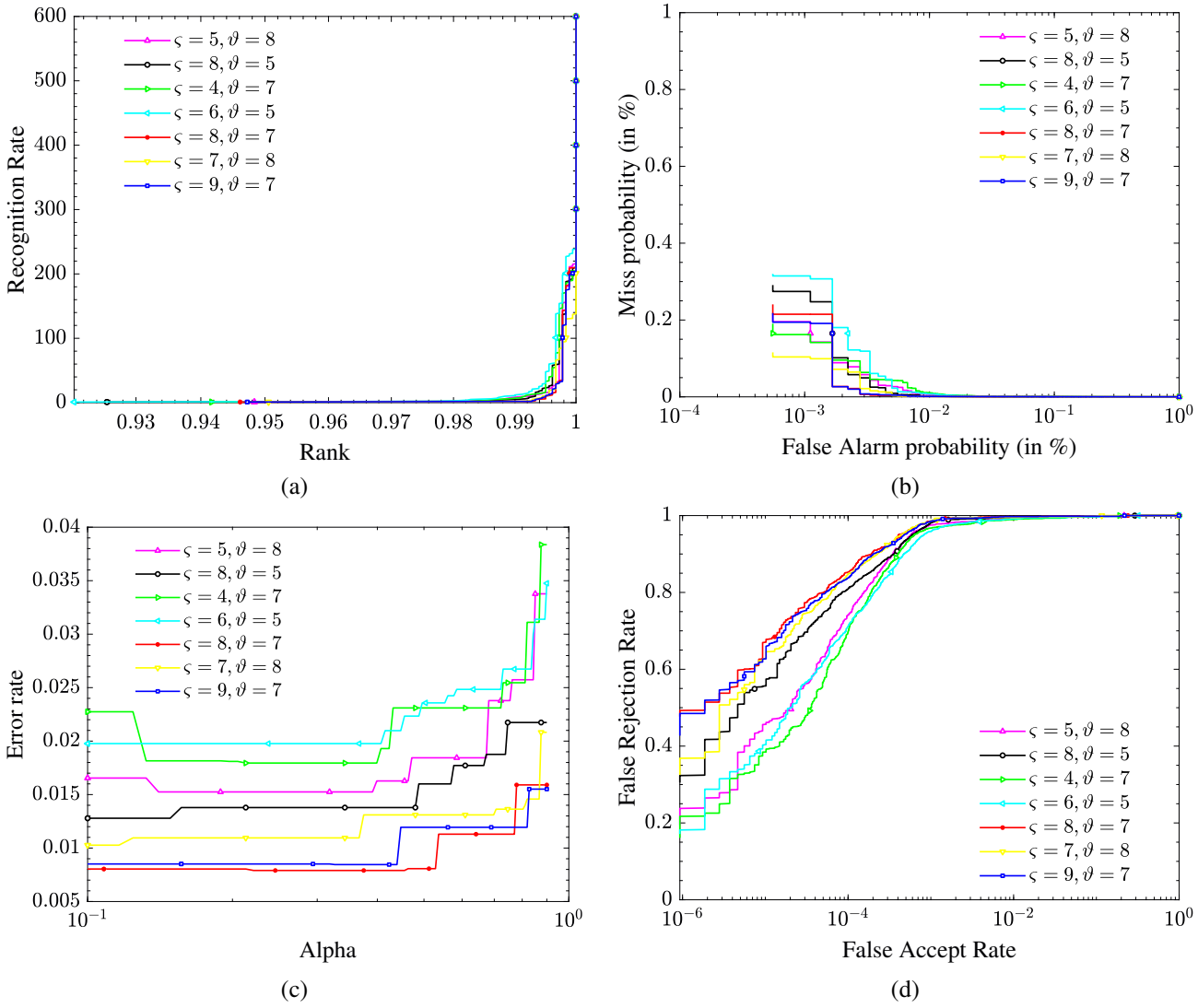

Fig. 4. Four types of biometric curves: (a) CMC, (b) DET, (c) EPC, and (d) ROC

recognition research outputs.The use of the $\varsigma = 8$ and $\vartheta = 7$ scale pairs Gabor gave the best research outcome compared to other value options. With this pair, we will get a verification value of $99,611\%$ and an error rate of 0.388% in the KPCA domain. The use of LDA has a good output value, but researchers are starting to abandon the dimensional reduction method because of the length of time the process takes. With four biometric curves ROC, EPC, DET, and CMC, it clarifies the advantages of using a series of methods: ThreeW, $[8 \times 7]$, KPCA, and cosine.

REFERENCES

[1] K. Bensid, D. Samai, F. Z. Laallam, and A. Meraoumia, "Deep learning feature extraction for multispectral palmprint identification," *Journal of Electronic Imaging*, vol. 27, no. 3, pp. 1 – 11, 2018. [Online]. Available: https://doi.org/10.1117/1.JEI.27.3.033018

[2] N. Saini and A. Sinha, "Efficient fusion of face and palmprint in gabor filtered wigner domain," *International Journal of Biometrics*, vol. 12, no. 3, pp. 301–316, 2020. [Online]. Available: https://www.inderscienceonline.com/doi/abs/10.1504/IJBM.2020.108482

[3] Y. Aberni, L. Boubchir, and B. Daachi, "Multispectral palmprint recognition: A state-of-the-art review," 07 2017, pp. 793–797.

[4] C. L. Deepika, A. Kandaswamy, C. Vimal, and B. Satish, "Palmprint authentication using modified legendre moments," *Procedia Computer Science*, vol. 2, pp. 164 – 172, 2010. [Online]. Available: http://www.sciencedirect.com/science/article/pii/S1877050910003510

[5] J. Sung, S.-Y. Bang, and S. Choi, "A bayesian network classifier and hierarchical gabor features for handwritten numeral recognition," *Pattern Recognition Letters*, vol. 27, no. 1, pp. 66 – 75, 2006. [Online]. Available: http://www.sciencedirect.com/science/article/pii/S0167865505001935

[6] H. jun Wang, H. nian Qi, and X. F. Wang, "A new Gabor based approach for wood recognition," *Neurocomputing*, vol. 116, pp. 192–200, 2013. [Online]. Available: http://dx.doi.org/10.1016/j.neucom.2012.02.045

[7] Q. Li, X. Li, Z. Guo, and J. You, "Online personal verification by palmvein image through palmprint-like and palmvein information," *Neurocomputing*, vol. 147, no. Supplement C, pp. 364 – 371, 2015, advances in Self-Organizing Maps Subtitle of the special issue: Selected Papers from the Workshop on Self-Organizing Maps 2012 (WSOM 2012). [Online]. Available: http://www.sciencedirect.com/science/article/pii/S0925231214008224

[8] G. S. Badrinath and P. Gupta, "Palmprint based recognition system using phase-difference information," *Future Generation Computer Systems*, vol. 28, no. 1, pp. 287–305, 2012. [Online]. Available: http://dx.doi.org/10.1016/j.future.2010.11.029

[9] M. Aykut and M. Ekinci, *Kernel Principal Component Analysis of Gabor Features for Palmprint Recognition*. Berlin, Heidelberg: Springer Berlin Heidelberg, 2009, pp. 685–694. [Online]. Available: https://doi.org/10.1007/978-3-642-01793-3_70

[10] Y. Xu, L. Fei, and D. Zhang, "Combining left and right palmprint images for more accurate personal identification," *IEEE Transactions on Image Processing*, vol. 24, no. 2, pp. 549–559, Feb 2015.

[11] C. A. Perez, L. A. Cament, and L. E. Castillo, "Methodological improvement on local gabor face recognition based on feature selection and enhanced borda count," *Pattern Recognition*, vol. 44, no. 4, pp. 951 – 963, 2011. [Online]. Available: //www.sciencedirect.com/science/article/pii/S0031320310005017

[12] Y. Xu, D. Zhang, and J.-Y. Yang, "A feature extraction method for use with bimodal biometrics," *Pattern Recognition*, vol. 43, no. 3, pp. 1106–1115, 2010. [Online]. Available: http://dx.doi.org/10.1016/j.patcog.2009.09.013

[13] B. Zhang, W. Li, P. Qing, and D. Zhang, "Palm-print classification by global features," *IEEE Transactions on Systems, Man, and Cybernetics: Systems*, vol. 43, no. 2, pp. 370–378, March 2013. [Online]. Available: http://dx.doi.org/10.1109/TSMCA.2012.2201465

[14] G. K. Ong Michael, T. Connie, and A. B. Jin Teoh, "A Contactless Biometric System Using Palm Print and Palm Vein Features," in *Advanced Biometric Technologies*. InTech, aug 2011. [Online]. Available: http://dx.doi.org/10.5772/19337

[15] I. Dokmanic, R. Parhizkar, J. Ranieri, and M. Vetterli, "Euclidean distance matrices: Essential theory, algorithms, and applications," *IEEE Signal Processing Magazine*, vol. 32, no. 6, pp. 12–30, Nov 2015.

[16] M. Velasquez and P. Hester, "An analysis of multi-criteria decision making methods," *International Journal of Operations Research*, vol. 10, pp. 56–66, 05 2013.

[17] A. Kumar and D. Zhang, "Palmprint authentication using multiple classifiers," in *Proceedings of SPIE - The International Society for Optical Engineering*, vol. 5404, 2004, pp. 20–29.

[18] K. Sudhakar and P. Nithyanandam, "An accurate facial component detection using gabor filter," *Bulletin of Electrical Engineering and Informatics*, vol. 6, no. 3, pp. 287–294, 2017.

[19] M. M. Hassan, H. I. Hussein, A. S. Eesa, and R. J. Mstafa, "Face recognition based on gabor feature extraction followed by fastica and lda," *Computers, Materials and Continua*, vol. 68, no. 2, pp. 1637–1659, 2021.

[20] R. Hammouche, A. Attia, S. Akhrouf, and Z. Akhtar, "Gabor filter bank with deep autoencoder based face recognition system," *Expert Systems with Applications*, p. 116743, 2022.

[21] X. Liang, J. Yang, G. Lu, and D. Zhang, "Compnet: Competitive neural network for palmprint recognition using learnable gabor kernels," *IEEE Signal Processing Letters*, vol. 28, pp. 1739–1743, 2021.

[22] X. Liang, Z. Li, D. Fan, J. Li, W. Jia, and D. Zhang, "Touchless palmprint recognition based on 3d gabor template and block feature refinement," *Knowledge-Based Systems*, vol. 249, p. 108855, 2022.

[23] V. Štruc and N. P. C, "Gabor-Based Kernel Partial-Least-Squares Discrimination Features for Face Recognition," *Informatica*, vol. 20, no. 1, pp. 115–138, 2009. [Online]. Available: http://iospress.metapress.com/index/173723327G3J5823.pdf

[24] H. jun Wang, H. nian Qi, and X.-F. Wang, "A new gabor based approach for wood recognition," *Neurocomputing*, vol. 116, pp. 192 – 200, 2013. [Online]. Available: http://www.sciencedirect.com/science/article/pii/S0925231212006881

[25] R. M. Haralick, K. Shanmugam, and I. Dinstein, "Textural features for image classification," *IEEE Transactions on Systems, Man, and Cybernetics*, vol. SMC-3, no. 6, pp. 610–621, Nov 1973. [Online]. Available: http://dx.doi.org/10.1109/TSMC.1973.4309314